

Maximum a posteriori estimation based wind fragility analysis with application to existing linear or hysteretic shear frames

Vincent Z. Wang* and John D. Ginger^a

School of Engineering and Physical Sciences, James Cook University,
Townsville, Queensland 4811, Australia

(Received November 16, 2013, Revised April 5, 2014, Accepted April 10, 2014)

Abstract. Wind fragility analysis provides a quantitative instrument for delineating the safety performance of civil structures under hazardous wind loading conditions such as cyclones and tornados. It has attracted and would be expected to continue to attract intensive research spotlight particularly in the nowadays worldwide context of adapting to the changing climate. One of the challenges encumbering efficacious assessment of the safety performance of existing civil structures is the possible incompleteness of the structural appraisal data. Addressing the issue of the data missingness, the study presented in this paper forms a first attempt to investigate the feasibility of using the expectation-maximization (EM) algorithm and Bayesian techniques to predict the wind fragilities of existing civil structures. Numerical examples of typical linear or hysteretic shear frames are introduced with the wind loads derived from a widely used power spectral density function. Specifically, the application of the maximum a posteriori estimates of the distribution parameters for the story stiffness is examined, and a surrogate model is developed and applied to facilitate the nonlinear response computation when studying the fragilities of the hysteretic shear frame involved.

Keywords: wind fragility analysis; hysteresis; missing data; EM algorithm; Bayesian statistics; maximum a posteriori estimation; surrogate model

1. Introduction

Strong wind loads may lead to significant economic and even life loss, as continually exhibited by numerous cyclones, hurricanes, and typhoons (Walker 1975, Boughton *et al.* 2011). Among various fast growing techniques, wind fragility analysis provides a quantitative instrument for dealing with the inherent uncertainty, and thus helps mitigate to some extent the risks associated with hazardous wind events (see, for example, Lee and Rosowsky 2006, and Rocha *et al.* 2011).

The performance of civil structures subject to hazardous wind loads can be assessed in a destructive way. Typically, this is achieved by loading corresponding scaled model structures, or full-scale model structures where appropriate, until one or more limit states of interest are reached. Destructive testing, if meticulously designed and conducted, could offer arguably the most straightforward mechanism through which the response of structures in reality can be studied.

*Corresponding author, Senior Lecturer, E-mail: vincent.wang@jcu.edu.au

^aAssociate Professor

Alternatively, more and more nondestructive testing procedures including structural health monitoring techniques (Chang 1997-2011, Chan and Thambiratnam 2011) have recently be formulated to carry out the performance assessment in such a way that no substantive damage will be introduced to the structures being tested, and even the interruption to the everyday operations relevant to the structures will be kept to a minimum.

As far as nondestructive testing procedures are concerned, a concomitant issue is that sometimes not all the structural appraisal data that are supposed to be collected actually turn out to be collected (Wang *et al.* 2014). The reasons for this include data acquisition system breakdowns, signal transmission errors, and vandalism and sabotage activities, to name but a few. Thereby, the challenge here is firstly how wind fragilities of an in-service structure can be evaluated when only incomplete appraisal data for the structure are available, and secondly, in terms of the final wind fragility evaluation results, how to achieve in an incomplete-data scenario a level of accuracy comparable (at least from some practical point of view) to that exhibited in the complete-data scenario.

In the following sections, the formulations of the two kinds of shear frame studied in this paper are first given, followed by the construction and validation of a surrogate model corresponding to the hysteretic shear frame. The wind fragility analysis scheme allowing for the possible missingness of some of relevant structural appraisal data is then detailed.

2. Configurations of two typical shear frames under wind loads

This section is organized as follows: The wind load model utilized in the study is presented in Subsection 2.1; Subsection 2.2 describes a linear three-story shear frame and a hysteretic two-story one, which are selected to illustrate the wind fragility analysis scheme to be elaborated in Section 4.

2.1 Wind loads

As the main objective of this study is to evaluate the wind fragilities using incomplete structural appraisal data, an established, representative wind load model in the literature (Soong and Grigoriu 1993, Simiu and Scanlan 1996) is chosen to synthesize the time varying wind loads. For the ease of reference and the completeness of presentation, the formulas and parameters used for the wind load synthesis are reviewed and reproduced below.

The power law is applied to determine the mean wind velocity u_h at the height h , as in Eq. (1) (Simiu and Scanlan 1996)

$$u_h = u_r \left(\frac{h}{h_r} \right)^\alpha \quad (1)$$

where u_r is the mean wind velocity at the reference height h_r , and α is a constant. Throughout the paper, the reference height h_r is taken to be 10 m with the corresponding mean wind velocity u_r being 50 m/s, and the constant exponent α is assumed to be 1/7. At a given height of h , $G(\omega)$, the one-sided power spectral density (PSD) function of the wind-induced excitation force acting at a surface area A normal to the direction of the wind, is shown by Eq. (2) (Soong and Grigoriu 1993, Simiu and Scanlan 1996)

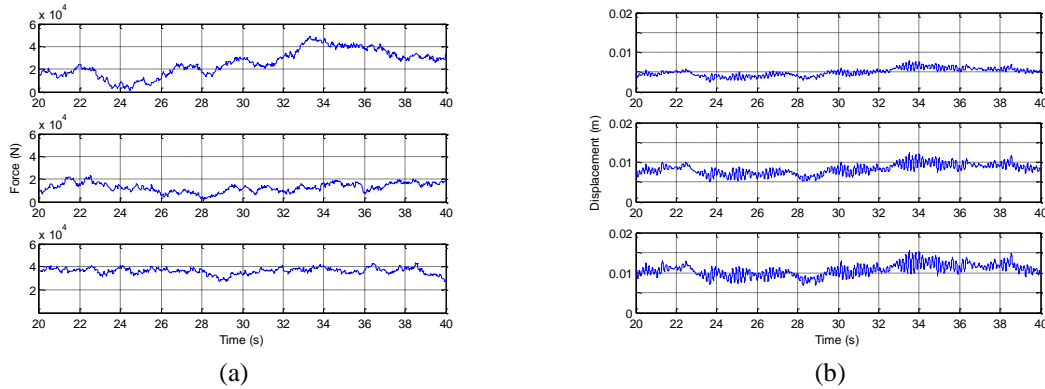


Fig. 1 For the linear three-story shear frame, the examples of (a) the wind-induced excitation-force time histories and (b) the corresponding displacement time histories at the first floor level (the two upper subfigures), the second floor level (the two middle subfigures), and the roof level (the two lower subfigures), where $h=5, 10$ or 15 m, respectively

$$G(\omega) = 0.52A^2 \rho^2 C_d^2 u_*^8 h^{-\frac{2}{3}} \omega^{-\frac{5}{3}} \tag{2}$$

where ω is the angular frequency; ρ is the air density; u_* is the friction velocity; and C_d is the drag coefficient. In this study, $A=10 \text{ m}^2$, $\rho=1.25 \text{ kg/m}^3$, $u_*=3.75 \text{ m/s}$, and $C_d=1.5$.

2.2 Linear or hysteretic shear frames

First, take a three-story shear frame as an example. Suppose that the shear frame can be modeled as a linear three-degree-of-freedom (DOF) system with its mass evenly lumped at the three floor/roof levels. Further assume that the shear frame has a uniform story height of 5 m. At the floor/roof levels, the wind-induced excitation-force time histories generated from the one-sided PSD function as in Eqs. (1) and (2) are illustrated in Fig. 1(a). Each story mass is considered as a deterministic quantity with its value equal to 2,000 kg, while a common trivariate normal distribution with all the three means, three variances, and six covariances respectively taken to be $1.5 \times 10^7 \text{ N/m}$, $2.025 \times 10^{13} \text{ N}^2/\text{m}^2$, and $1.0125 \times 10^{13} \text{ N}^2/\text{m}^2$ is used to simulate both the complete and incomplete structural appraisal data for the story stiffnesses. These parameter values for the probability distribution correspond to a coefficient of variation of 0.3 for any of the three story stiffnesses and a correlation coefficient of 0.5 between any two of them. Also, denote the first, second, and third story stiffnesses by K_1 , K_2 , and K_3 , respectively. Corresponding to the excitation forces described in Fig. 1(a), Fig. 1(b) shows an example of the displacement time histories obtained at the floor/roof levels.

In the context of inelastic analysis of civil structures, the phenomenon of hysteresis is an important, perhaps inevitable issue that needs to be appropriately taken into account. The hysteresis phenomenon can be described by various plasticity models in which hysteresis manifests itself in the constitutive relations of the materials involved. Alternatively, the phenomenon may also be allowed for at the structural system level, as investigated by Mostaghel (1999) and Mostaghel and Byrd (2000), among other researchers. The relative effectiveness and

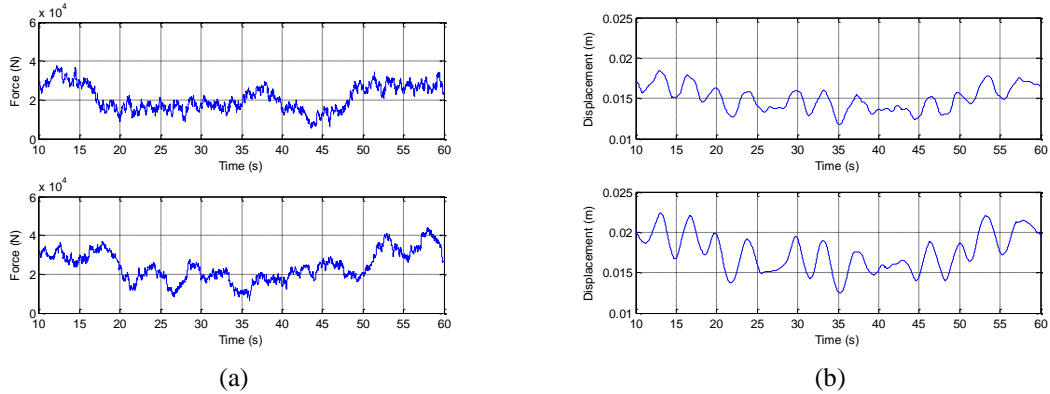


Fig. 2 For the hysteretic two-story shear frame, the examples of (a) the wind-induced excitation-force time histories and (b) the corresponding displacement time histories at the first floor level (the two upper subfigures) and the roof level (the two lower subfigures), where $h = 7.5$ or 15 m, respectively

convenience of these two kinds of description are highly problem-specific, and moreover it is worth noting that in some cases the boundary between them could blur.

A two-story nonlinear hysteretic shear frame as described by Mostaghel (1999) and Mostaghel and Byrd (2000) is used to illustrate the wind fragility analysis scheme to be proposed in this study. The equations of motion of the frame are shown in Eqs. (3)-(6)

$$\mathbf{M}\ddot{\mathbf{U}}(t) + \mathbf{C}\dot{\mathbf{U}}(t) + \gamma\mathbf{K}'\mathbf{U}(t) + (1-\gamma)\mathbf{K}''\mathbf{V}(t) = \mathbf{F}_w(t) \quad (3)$$

$$\dot{\mathbf{V}}(t) = \mathbf{G}(\mathbf{U}(t), \mathbf{V}(t), \dot{\mathbf{U}}(t), \dot{\mathbf{V}}(t))\dot{\mathbf{U}}(t) \quad (4)$$

in which

$$\mathbf{K}' = \begin{pmatrix} K_1 + K_2 & -K_2 \\ -K_2 & K_2 \end{pmatrix} \quad (5)$$

$$\mathbf{K}'' = \begin{pmatrix} K_1 & -K_2 \\ 0 & K_2 \end{pmatrix} \quad (6)$$

where t is the time; \mathbf{M} is the lumped mass matrix; \mathbf{C} is the damping matrix; \mathbf{K}' and \mathbf{K}'' are the stiffness matrix and the auxiliary stiffness matrix, respectively; $\mathbf{F}_w(t)$ is the wind-induced excitation-force time history; $\mathbf{U}(t)$ is the displacement time history; the parameter γ is known as the post-yield-to-pre-yield stiffness ratio; and K_1 and K_2 respectively denote the story stiffness for the first story and that for the second story. Notice that, by some abuse of notation, K_1 and K_2 , which are originally introduced to denote the story stiffnesses for the linear shear frame, now also refer to the corresponding quantities for the hysteretic shear frame. For the hysteretic shear frame being considered, the equations of motion contain a total of four unknown functions, i.e., the four components of $\mathbf{U}(t)$ and $\mathbf{V}(t)$. \mathbf{G} is a function of $\mathbf{U}(t)$, $\mathbf{V}(t)$, $\dot{\mathbf{U}}(t)$, and $\dot{\mathbf{V}}(t)$, and its specific expression can be found in Mostaghel (1999) and Mostaghel and Byrd (2000). The story stiffnesses K_1 and K_2 are assumed to have a bivariate normal distribution with both of the means

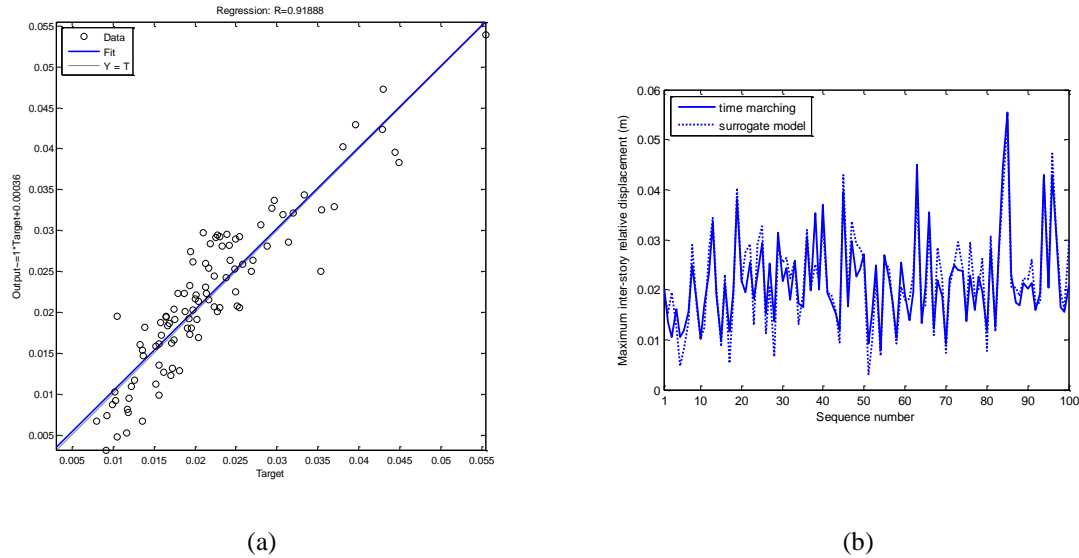


Fig. 3 Validation of the constructed surrogate model: (a) Regression analysis of the maximum inter-story relative displacements obtained from the surrogate model on those from the time marching procedures; and (b) comparison between the maximum inter-story relative displacements resulting from the surrogate model and those from the time marching

being 1×10^7 N/m, both of the variances being 2.25×10^{12} N²/m², and a covariance of 1.125×10^{12} N²/m². These parameter values are in accordance with both the coefficients of variation equal to 0.15 and a correlation coefficient of 0.5. Further, assume that both of the diagonal entries of \mathbf{M} are 1.25×10^6 kg, and that the parameter γ is equal to 0.15. Using a uniform story height of 7.5 m, the wind-induced excitation force $\mathbf{F}_w(t)$ can be simulated based on the representative wind load model as documented by Soong and Grigoriu (1993) and Simiu and Scanlan (1996) and reviewed in Subsection 2.1. Fig. 2(a) illustrates the simulated $\mathbf{F}_w(t)$ for a height h of 7.5 m (i.e., the first floor level) or 15 m (i.e., the roof level). Corresponding to a set of $\mathbf{F}_w(t)$ data, some well-established time marching procedures are readily available to compute the displacement time history $\mathbf{U}(t)$. For example, Fig. 2(b) shows the $\mathbf{U}(t)$ values obtained by using the classical fourth-order Runge-Kutta algorithm. The maximum inter-story relative displacement, an important quantity in structural safety assessment, can then be computed.

3. Surrogate-model construction and validation

Once the hysteresis description is selected and the structural equilibrium equation, which could be static or dynamic, is set up, the structural response can then be computed. Conceptually this process sounds fairly natural and smooth, while practically it may result in prolonged computation time, which could at worst become a prohibitive inconvenience especially when the process is to serve as a subroutine to be frequently called in a larger algorithm. For instance, in a Monte Carlo simulation based reliability analysis, it is not uncommon for the process to be repeated thousands of times. With strong wind loads identified as a kind of extreme load, this section is thus

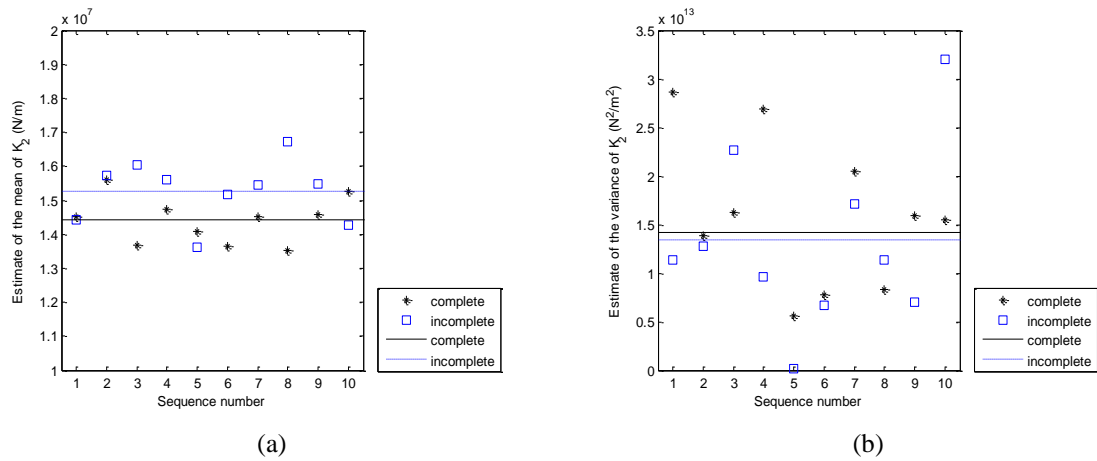


Fig. 4 Estimates of (a) the mean and (b) variance of K_2 in the complete- and incomplete-data scenarios for the linear three-story shear frame, with the relevant averages marked by the horizontal lines

concerned with the efficient wind response computation of the typical hysteretic shear frame shown in Section 2. Specifically, a surrogate model is developed to replace some conventional time marching procedures. Then in the fourth section the surrogate model is applied to assess the safety performance of the hysteretic structure, and due consideration is given to the relevant data missingness events that could occur during structural appraisal activities in reality.

In order to construct a surrogate model to determine the maximum inter-story relative displacement in a more efficient way, a feedforward backpropagation neural network is created and trained. The database used for the neural network training is formed by 2,000 independent runs of the fourth-order Runge-Kutta algorithm, and for each run the time marching stops at $t=60$ s. When training the neural network, each of the 2,000 sets of the input data sequentially comprises the two story stiffnesses, the sampled (sampling rate: 1/50) excitation-force time history at the first floor level, and that at the roof level, and each of the output data is the maximum inter-story relative displacement. With the fourth-order Runge-Kutta algorithm chosen as the benchmark time marching procedures, the resulting trained neural network is then independently validated, as in Fig. 3. It can be observed that the maximum inter-story relative displacement values yielded by the trained neural network agree with those from the time marching procedures reasonably well.

4. Wind fragility analysis based on relevant maximum a posteriori estimates

The section is organized as below: Subsection 4.1 is from a frequentist perspective, and the two typical shear frames are used as examples to introduce some expectation-maximization (EM) algorithm (Dempster *et al.* 1977, Wu 1983, Meng and van Dyk 1997) based wind fragility evaluation procedures. The procedures are then validated by the comparisons between the wind fragilities obtained in the incomplete-data scenario and the corresponding results in the complete-data scenario. The potential of a Bayesian approach for wind fragility evaluation is then explored in Subsection 4.2.

Table 1 An example of the incomplete structural appraisal data for the linear three-story shear frame

Story ID	Incomplete structural appraisal data for the story stiffness ($\times 10^7$ N/m)
1	1.7843; 1.8050; NA; 1.4833; NA; 2.0190; 1.8119; 2.0233; NA; 1.6220; 1.0276; NA; NA; NA; NA; 2.0829; 1.8250; 1.6292; NA; NA; 0.8409; 1.3106; 1.7182; NA; 1.6078; 1.7673; 1.5995; NA; 0.7471; NA.
2	1.2363; 1.6302; 1.2494; 1.8557; 1.0746; 1.1058; NA; NA; 0.7130; NA; 1.6557; 1.4519; 1.4944; 0.9117; 1.7041; 2.1901; 1.3980; 1.4777; 1.4856; 1.0454; NA; 1.6080; NA; 1.4439; NA; 1.7750; NA; 1.8832; 1.4319; NA.
3	NA; 1.7167; 1.0266; 1.7964; 0.9410; 1.5674; 1.8447; 1.4013; 1.2851; 1.7263; 1.2698; 0.7939; 2.1242; 1.9900; 1.7958; NA; 2.0807; NA; 1.0034; 1.8905; NA; 2.0350; NA; 1.8023; NA; 1.7116; 1.6808; NA; 0.7966; NA.

Note: An “NA” denotes a missing data point, which also applies to Table 3.

Table 2 Estimated wind fragilities in Cases I and II

Case ID	Estimated wind fragilities
I	0.421; 0.500; 0.506; 0.478; 0.585; 0.637; 0.516; 0.573; 0.490; 0.474.
II	0.422; 0.321; 0.451; 0.510; 0.520; 0.380; 0.493; 0.414; 0.430; 0.526.

4.1 Validation: a frequentist perspective

Throughout this study, in the incomplete-data scenario the missingness pattern is assumed to follow the missing-completely-at-random manner (Heitjan and Basu 1996), and a missingness probability of 0.3 is assigned to each appraisal data point.

For the linear shear frame, Table 1 as an example lists some appraisal data in the incomplete-data scenario. For the fragility analysis in this study, failure of the shear frame is defined as the situation when the maximum inter-story relative displacement exceeds a pre-selected threshold U_m , and the fragility is quantified by the probability of this failure event. In this subsection, U_m is chosen to be 0.01 m for the linear shear frame. To deal with the incomplete appraisal data for the story stiffness, the EM algorithm is implemented through the statistical computing environment *R* (*R* Core Team 2012) and the package *norm* (Novo and Schafer 2012). To validate results obtained in the incomplete-data scenario, the following scheme is designed: In the incomplete-data scenario, the 1,000-time Monte Carlo simulation is independently carried out ten times, yielding a sample containing ten realizations of the fragility. In parallel, another fragility sample is constructed in the complete-data scenario. The null hypothesis that these two samples are from a same population is then tested against the alternative hypothesis that their populations are different from each other. Accordingly, one may expect that the null hypothesis cannot be rejected if the procedures used to deal with the appraisal data missingness are deemed effective. The above validation scheme leads to the estimates illustrated in Fig. 4 and the fragilities shown in Table 2, where Cases I and II respectively correspond to the complete- and incomplete-data scenarios. For the data in Table 2, the null hypothesis cannot be rejected based on the two-sample Kolmogorov-Smirnov test at a commonly used significance level of 0.05.

Consider the hysteretic two-story shear frame defined in Section 2. Suppose that the frame has been in service for a period of time, and its in-situ story stiffnesses K_1 and K_2 need to be evaluated using structural appraisal techniques. Table 3 gives an example of some incomplete structural appraisal data. As mentioned previously, it is assumed that the relevant appraisal data points are missing completely at random, and the missingness probability is 0.3. Again, the EM algorithm

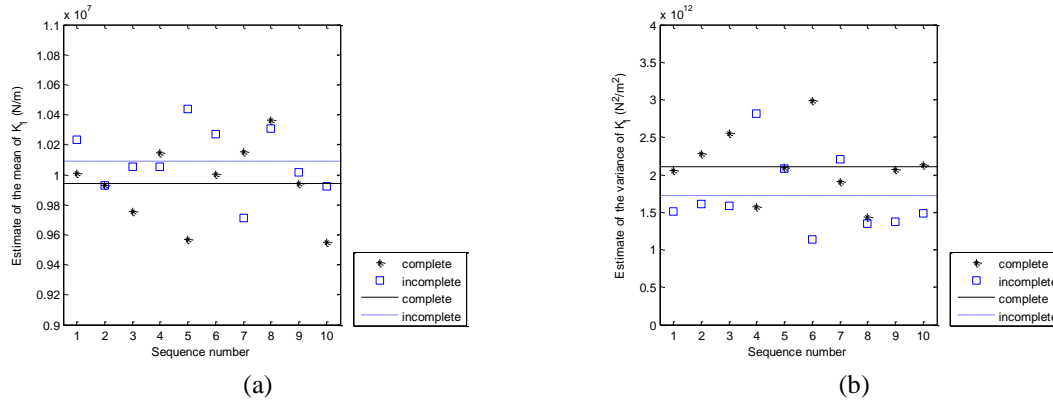


Fig. 5 Estimates of (a) the mean and (b) variance of K_1 in the complete- and incomplete-data scenarios for the hysteretic two-story shear frame, with the relevant averages marked by the horizontal lines

Table 3 An example of the incomplete structural appraisal data for the hysteretic two-story shear frame

Story ID	Incomplete structural appraisal data for the story stiffness ($\times 10^7$ N/m)
1	0.9790; 0.8685; 0.9251; 1.1092; 1.1283; 0.7588; NA; 0.9295; 1.0301; 1.0156;
	1.0684; 1.0402; NA; NA; NA; 1.0641; NA; 0.9946; 1.0817; NA;
	1.0843; 0.9329; 1.2423; 0.8932; 1.0120; 1.2727; 1.0925; NA; 0.8282; 1.1834.
2	1.2293; 0.9902; 0.7541; NA; NA; NA; 1.0702; 1.1302; NA; NA;
	1.0836; 1.1869; 1.0253; 0.9788; 0.9552; NA; NA; NA; 0.9465; 0.9008;
	1.1277; NA; NA; NA; NA; 0.8916; 1.2934; 1.2529; 1.0118; 0.9083.

Table 4 Estimated wind fragilities in Cases III and IV

Case ID	Estimated wind fragilities
III	0.623; 0.623; 0.659; 0.586; 0.682; 0.571; 0.569; 0.533; 0.638; 0.702.
IV	0.567; 0.645; 0.595; 0.566; 0.507; 0.556; 0.680; 0.508; 0.579; 0.657.

can be applied to deal with the appraisal data missingness. Along with the surrogate model developed in Section 3 and the threshold U_m of 0.02 m, the wind safety of this in-service shear frame can then be assessed. Indeed, as in Fig. 5 and Table 4, the scheme is effective in the sense that, corresponding to the estimated wind fragilities in the constructed complete- and incomplete-data scenarios, no significant difference is signaled by the two-sample Kolmogorov-Smirnov test with a significance level of 0.05. Notice that in Table 4 the estimated wind fragilities in Cases III and IV refer to the wind fragilities computed in the complete- and incomplete data scenarios, respectively.

4.2 Implementation: a Bayesian approach

Bayesian techniques together with their application to civil engineering form an intriguing family of procedures thanks to their general capacity of systematically taking into account cognate prior information. As a preliminary attempt to explore the potential application of Bayesian techniques to the analysis of wind fragilities with incomplete structural appraisal data, a normal

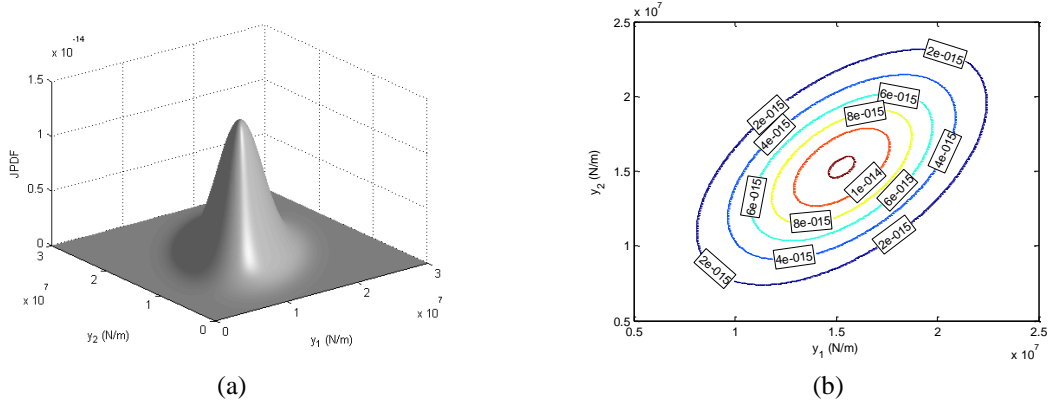


Fig. 6 For the linear three-story shear frame in the incomplete-data scenario, (a) the estimated JPDF of K_1 and K_2 based on the averages of the relevant maximum a posteriori estimates, and (b) the contour plot of the estimated JPDF shown in (a)

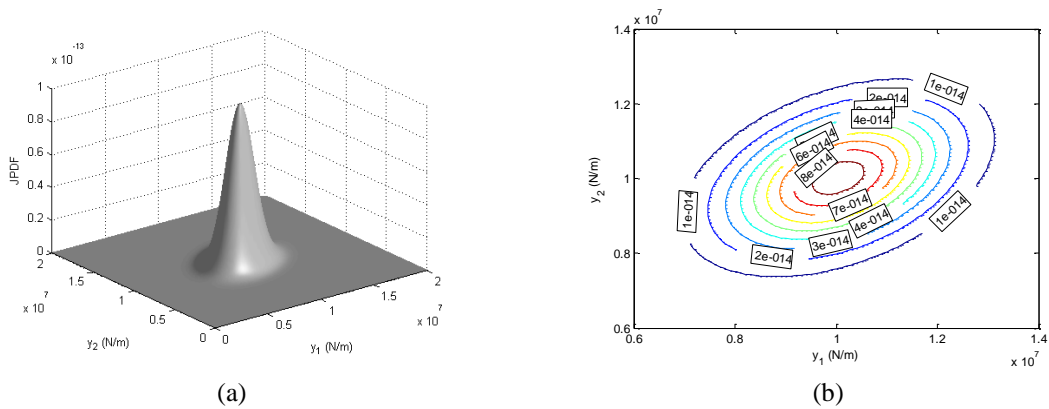


Fig. 7 For the hysteretic two-story shear frame in the incomplete-data scenario, (a) the estimated JPDF of K_1 and K_2 based on the averages of the relevant maximum a posteriori estimates, and (b) the contour plot of the estimated JPDF shown in (a)

Table 5 Estimated wind fragilities in Cases V and VI

Case ID	Estimated wind fragilities
V	0.739; 0.684; 0.780; 0.622; 0.676; 0.697; 0.819; 0.725; 0.708; 0.657.
VI	0.297; 0.173; 0.324; 0.193; 0.216; 0.118; 0.286; 0.251; 0.261; 0.183.

inverse Wishart distribution, which is a conjugate prior distribution in this context, is selected to model the mean vector and the covariance matrix of the story stiffnesses. Specifically, Figs. 6 and 7 respectively describe the estimated joint probability density function (JPDF) of the story stiffnesses K_1 and K_2 for the linear and hysteretic shear frames in the incomplete-data scenario. Each of these two plotted JPDFs results from ten sets of relevant incomplete structural appraisal data and the averages of the corresponding maximum a posteriori estimates of the means,

Table 6 Estimated wind fragilities in Cases VII and VIII

Case ID	Estimated wind fragilities
VII	0.892; 0.804; 0.746; 0.858; 0.773; 0.811; 0.744; 0.733; 0.818; 0.859.
VIII	0.418; 0.364; 0.401; 0.410; 0.287; 0.392; 0.345; 0.346; 0.373; 0.424.

variances, and covariances of the story stiffnesses. With the threshold U_m for the linear shear frame chosen to be 0.008 m and 0.012 m in Cases V and VI respectively, the estimated wind fragilities in the incomplete-data scenario are listed in Table 5. Similar situations for the hysteretic shear frame are also investigated, where the threshold U_m is 0.015 m for Case VII while 0.025 m for Case VIII. The final results of the estimated wind fragilities are summarized in Table 6. It can be observed that, with a more stringent threshold in Case V or VII than in Case VI or VIII respectively, the resulting wind fragilities increase considerably.

5. Conclusions

Primarily, the study presented in this paper lays the groundwork for further investigation into the appropriate incorporation of relevant prior information into the evaluation of the safety performance of civil structures against hazardous wind loads. The prior information under the current circumstances could come from code specifications, design experience, and previously conducted structural appraisal activities, among other sources. As an example, the study particularly focuses on the wind fragility range that is of practical importance to weighing up on a large scale the implications resulting from hazardous wind loads. This is the range that an insurance company, for instance, may be concerned with when evaluating its financial positions related to a hazardous wind event. It is also the range within which a government agency often needs detailed, quantitative results when working out the level of post-hazard relief package to be committed. Meanwhile, it should be noted that the wind fragilities that a structural engineer may have to deal with in an analysis-and-design task can sometimes fall well below the range investigated in this study. The performance of the proposed methodology in determining those wind fragilities thus warrants further research effort.

As a by-product during the wind fragility investigation, a surrogate model useful for improving the efficiency in the response computation of a typical hysteretic structure under wind loads is also designed in this paper. The nonlinear response of civil structures is often characterized by the phenomenon of hysteresis. The ongoing research effort in relevant topics has been generating scores of analytical descriptions corresponding to a number of nonlinear hysteretic systems. Nevertheless, many conventional time integration procedures associated with these descriptions can be arduous. Focusing on a typical description, this paper presents the development of a surrogate model in place of the conventional procedures with the aim of improving the time integration efficiency. In particular, the performance of the surrogate model is demonstrated by studying the nonlinear response of the hysteretic system due to wind loads. The application of the surrogate model to the structural safety assessment is illustrated as well. It is expected that models of this kind could be combined with other pertinent techniques to better assess the wind safety performance of a broad range of in-service civil structures.

Acknowledgements

The technical support obtained from the Cyclone Testing Station (<https://www.jcu.edu.au/cts/>) at James Cook University is greatly acknowledged.

References

- Boughton, G.N., Henderson, D.J., Ginger, J.D., Holmes, J.D., Walker, G.R., Leitch, C.J. *et al.* (2011), *Tropical Cyclone Yasi Structural Damage to Buildings - Technical Report No. 57*, Cyclone Testing Station, James Cook University, Australia.
- Chan, T. and Thambiratnam, D.P. (2011), *Structural Health Monitoring in Australia*, Nova Science Publishers, Hauppauge, NY.
- Chang, F.K. (1997-2011), *Proceedings of the 1st-8th International Workshops on Structural Health Monitoring*, Stanford, CA.
- Dempster, A.P., Laird, N.M. and Rubin, D.B. (1977), "Maximum likelihood from incomplete data via the EM algorithm", *J. R. Stat. Soc. Ser. B - Methodol.*, **39**(1), 1-38.
- Heitjan, D.F. and Basu, S. (1996), "Distinguishing 'missing at random' and 'missing completely at random'", *Am. Stat.*, **50**(3), 207-213.
- Lee, K.H. and Rosowsky, D.V. (2006), "Fragility curves for woodframe structures subjected to lateral wind loads", *Wind Struct.*, **9**(3), 217-230.
- Meng, X.L. and van Dyk, D. (1997), "The EM algorithm - an old folk-song sung to a fast new tune", *J. R. Stat. Soc. Ser. B - Methodol.*, **59**(3), 511-567.
- Mostaghel, N. (1999), "Analytical description of pinching, degrading hysteretic systems", *J. Eng. Mech., ASCE*, **125**(2), 216-224.
- Mostaghel, N. and Byrd, R.A. (2000), "Analytical description of multidegree bilinear hysteretic system", *J. Eng. Mech., ASCE*, **126**(6), 588-598.
- Novo, A.A. and Schafer, J.L. (2012), *Norm: Analysis of Multivariate Normal Datasets with Missing Values*, R Package Version 1.0-9.4, <http://CRAN.R-project.org/package=norm>.
- R Core Team (2012), *R: A Language and Environment for Statistical Computing*, R Foundation for Statistical Computing, Vienna, Austria, ISBN 3-900051-07-0, <http://www.R-project.org>.
- Rocha, D., Eamon, C.D. and Murphy, J.F. (2011), "Reliability analysis of roof sheathing panels exposed to a hurricane wind", *Struct. Saf.*, **33**(1), 74-81.
- Simiu, E. and Scanlan, R.H. (1996), *Wind Effects on Structures: Fundamentals and Applications to Design*, 3rd Edition, John Wiley & Sons, New York, NY.
- Soong, T.T. and Grigoriu, M. (1993), *Random Vibration of Mechanical and Structural Systems*, Prentice Hall, Englewood Cliffs, NJ.
- Walker, G.R. (1975), *Report on Cyclone "Tracy": Effect on Buildings, December 1974*, Department of Housing and Construction, Australia.
- Wang, V.Z., Mallett, M. and Priory, A. (2014), "Seismic fragility evaluation with incomplete structural appraisal data: an iterative statistical approach", *J. Struct. Eng., ASCE*, **140**(2), Paper ID 04013048, 13.
- Wu, C.F.J. (1983), "On the convergence properties of the EM algorithm", *Ann. Stat.*, **11**(1), 95-103.

Notation

- A : Surface area normal to the direction of the wind
 C : Damping matrix for the hysteretic shear frame
 C_d : Drag coefficient

$\mathbf{F}_w(t)$: Wind-induced excitation-force time history for the hysteretic shear frame
\mathbf{G}	: Function used in the equation of motion of the hysteretic shear frame
$G(\omega)$: One-sided power spectral density function of a wind-induced excitation force
h	: Height
h_r	: Reference height
\mathbf{K}'	: Stiffness matrix for the hysteretic shear frame
\mathbf{K}''	: Auxiliary stiffness matrix for the hysteretic shear frame
K_i	: Random variable denoting the i th story stiffness for the linear or hysteretic shear frame
\mathbf{M}	: Lumped mass matrix for the hysteretic shear frame
t	: Time
U_m	: Threshold for the maximum inter-story relative displacement
$\mathbf{U}(t)$: Displacement time history for the hysteretic shear frame
u_*	: Friction velocity
u_h	: Mean wind velocity at the height h
u_r	: Reference wind velocity at the reference height h_r
$\mathbf{V}(t)$: Unknown function in addition to $\mathbf{U}(t)$ in the equation of motion of the hysteretic shear frame
α	: Constant exponent in the power law used to determine the mean wind velocity u_h
γ	: Post-yield-to-pre-yield stiffness ratio for the hysteretic shear frame
ρ	: Air density
ω	: Angular frequency as the argument of the function $G(\omega)$